

Measurement of the Number of Muons in Inclined Showers at the Pierre Auger Observatory

M. Oliveira, L. Cazon, M. Pimenta
Dep. Physics, IST, Lisbon, Portugal
LIP, Lisbon, Portugal

July 20, 2012

Abstract

The field of extreme energy cosmic rays was born with the detection of an air shower corresponding to a primary particle having an energy of about 10^{20} eV at the Volcano Ranch experiment in 1962. While the origin and acceleration mechanisms of the ultra-high-energy cosmic particles remain a challenging astrophysical question, the nature of these particles and their interactions in the atmosphere address fundamental particle physics questions. The centre-of-mass energies involved in these interactions are more than one order of magnitude above those reached at the LHC. Extreme energy cosmic rays are the only possibility to explore the 100 TeV energy scale in the years to come. Such an exploration involves the understanding of the electromagnetic, muon and light components of air showers in the next generation of high-energy cosmic ray experiments. This work starts with a synthesis of the field of Ultra High Energy Cosmic Rays. The Pierre Auger Observatory is described in detail and an overview of its most important results is given. The main focus of this work is on the direction of breaking the degeneracy between hadronic interaction models and mass composition determination. In a first approach we show that the hadronic models do not fit the recent Auger data well by putting the emphasis on the muonic content of air showers. In the final part of this work we develop a new, original method for measuring the number of muons in extensive air showers on the ground. An application to Auger data is performed and the results are compared to the predictions of hadronic models.

Keywords: Ultra High energy Cosmic Rays, Pierre Auger Observatory, Extensive Air Showers, Hadronic Models, Muons.

1 Introduction

This work is focused on Ultra High energy Cosmic Rays (UHECR) and some of their properties, precisely the study of their composition and its degeneracy with different hadronic interaction models. The first part of the work, deals with the physics of UHECRs, description of their spectrum, study of their origin, propagation and detection at Earth. A detailed description of the Pierre Auger Observatory is given, the main detectors composing the observatory and the reconstruction tech-

niques of events are also described. Furthermore the main results obtained with the Pierre Auger Observatory are described. In this work we have studied two shower observables X_{\max} and N_{μ} in order to retrieve new properties on the primary CR mass composition and new information on the hadronic interaction models. An important emphasis is given to the number of muons N_{μ} in order to show its importance in the mass composition and hadronic model studies. Finally we propose a new way of measuring the number of muons on the ground from the signal in the surface detector.

A description of the method is given, its main features are discussed and an application to data is performed. Finally we conclude the work by commenting the main results obtained and give prospects for future studies.

2 Recent Results

The Pierre Auger Observatory (PAO) is the largest existing experiment for measuring UHECRs. It has acquired more statistics than any other previous experiment. Auger was able to measure the UHECR spectrum with unprecedented statistics [5], allowing to observe the ankle structure and the cutoff at the end of the spectrum. Figure 1 shows the results of HiRes and Auger combined. The two spectra present the same main features, with the ankle structure and the cutoff. The difference between the two spectra are within the systematic uncertainties of both experiments.

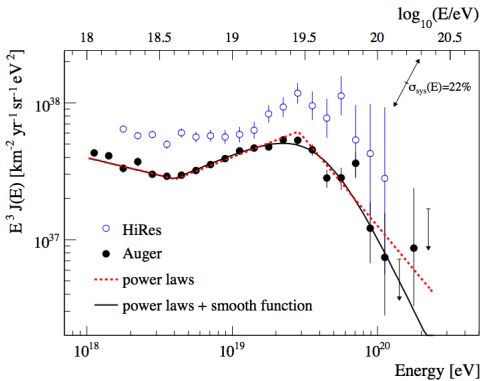


Figure 1: UHECR energy spectrum measured by Auger (black dots) and by HiRes (blue dots) experiments. The flux is scaled by E^3 to emphasize the features of the spectrum. The ankle and the GZK cutoff can be observed. The systematic uncertainty of the Auger energy scale of 22% is indicated by the arrows [5].

Another important result from the PAO is the measurement of the number of muons on the ground. The number of muons is a powerful observable that could serve as a composition discriminator. The number of muons measured in the data is well above the number of muons predicted by the hadronic interaction models. Figure 2 from [6] represents the number of muons from various Auger events compared with reference lines for *EPOS* iron (the model that predicts the larger number of muons) and for *QGSJETII* proton. This result

emphasizes the inability of the hadronic models to describe the number of muons. These models need to be updated in order to best fit the real data.

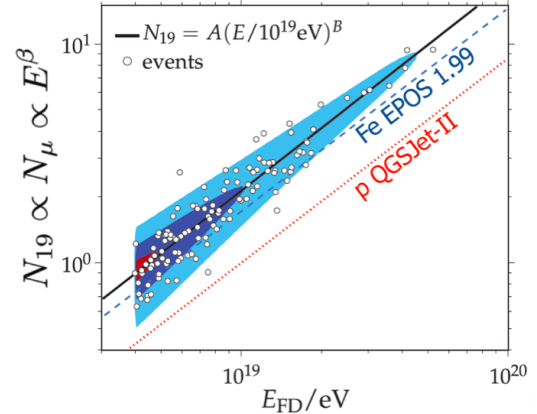


Figure 2: Number of muons from Auger data [6]. This number was determined using the golden method. The line corresponds to a fit of the calibration curve $N_{19} = A(E/10^{19} \text{ eV})^B$, where the constants A and B are obtained using the maximum likelihood method. The dotted line corresponds to the calibration curve for proton *QGSJETII* and the dashed line corresponds to the calibration curve of iron *EPOS*.

3 Joint interpretation of X_{max} and N_{μ}

The nature of the UHECR remains an open question in physics. Data from the Pierre Auger Collaboration can be interpreted as a gradual increase in the average mass number of the primary incoming cosmic ray with increasing energy. The mass composition of UHECR is a long standing puzzle in physics. The mass of the primary CR can provide important constraints on the acceleration of CRs and on their propagation. In order to study the mass composition of UHECR one cannot use the energy spectrum due to the scarce data, the uncertainties on the galactic and extragalactic magnetic fields and to the distribution of the sources. At the PAO the study of mass composition is performed through the study of the shower characteristics. Shower variables like the X_{max} and $\text{RMS}(X_{\text{max}})$ have been used in order to infer the mass properties of the most energetic particles ever detected. The evolution of $\langle X_{\text{max}} \rangle$,

also known as the elongation rate is used to study composition. The X_{\max} varies with composition, heavier showers will interact earlier in the atmosphere, thus penetrate less than showers with a smaller number of nucleons A . Figure 3 depicts the evolution of X_{\max} with the energy from the results obtained by the PAO. The data seems to indicate a transition from lighter to heavier elements with the energy. Apart from the X_{\max} one can also use the $\text{RMS}(X_{\max})$ to study composition. Showers with a larger A produce more secondary particles and thus fluctuate less, making $\text{RMS}(X_{\max})$ a good observable in the study of mass composition. In figure 3 one can see the evolution of X_{\max} with the energy. Both X_{\max} and $\text{RMS}(X_{\max})$ seem to indicate a change in composition from proton to iron at the highest energies.

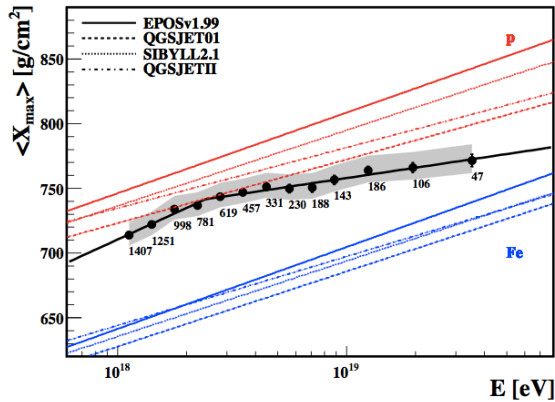


Figure 3: Recent data for X_{\max} from [4]. Data points are shown with the systematic error bars. The lines correspond to the predictions for p and Fe primaries from different hadronic interaction models. The number of events in each bin is indicated.

3.1 Transition to Iron

In this section we discuss two different approximated scenarios with a two component transition from proton to iron. The relative abundance of iron nuclei $\alpha(E)$ is set to evolve linearly with the logarithm of the energy $\log_{10}(E)$.

The dependence on α for both $\langle X_{\max} \rangle$ and

$\text{RMS}(X_{\max})$ can be expressed as:

$$\langle X_{\max} \rangle(\alpha) = (1 - \alpha) \langle X_{\max} \rangle_p + \alpha \langle X_{\max} \rangle_{Fe} \quad (1)$$

$$\begin{aligned} \text{RMS}^2(X_{\max})(\alpha) &= (1 - \alpha) \text{RMS}^2(X_{\max})_p \quad (2) \\ &+ \alpha \text{RMS}^2(X_{\max})_{Fe} \\ &+ \alpha(1 - \alpha) \left(\langle X_{\max} \rangle_p - \langle X_{\max} \rangle_{Fe} \right)^2 \end{aligned}$$

where the subscripts p and Fe label the averages and RMS of pure proton and iron primaries respectively. The same equation would also stand for the number of muons N_μ , by substituting $\langle X_{\max} \rangle$ by $\langle N_\mu \rangle$ and $\text{RMS}(X_{\max})$ by $\text{RMS}(N_\mu)$.

The shower simulations were produced using CONEX: 50 000 proton and iron induced showers for each energy ($E \in [10^{18}, 10^{20}]$ eV). All the showers were generated with a fixed zenith angle $\theta = 40^\circ$.

3.2 Cross Section change hypothesis

In the following scenario, we have modified in two different ways the values of all the hadronic cross-sections within CONEX for the QGSJETII model above $10^{18.5}$ eV. More specifically we modified the FORTRAN subroutine QGSSIGMAII with a function of the energy $f(E)$ that we obtained fitting the points given in [7]. Figure 4 displays the modified cross-sections obtained with two different functions $f(E)$. The values for $f(E)$ are motivated by the cross section measurements obtained in [7] and [8].

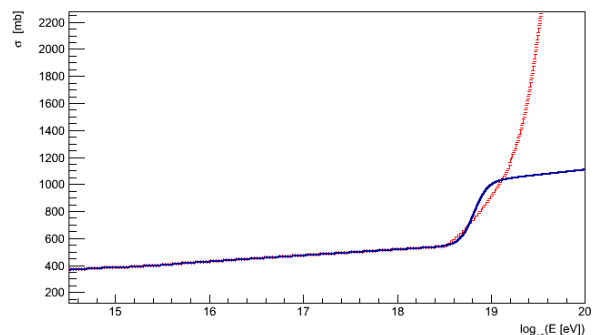


Figure 4: Cross-sections models used to describe the $\text{RMS}(X_{\max})$ data as a function of primary energy. Below $E = 10^{18.5}$ eV we used the cross section of QGSJETII. Above this energy two hypothesis were tested: a fast evolution to a black disk [8] in blue; and a very fast continuous increase (in red).

4 N_μ on the ground at $\theta = 60^\circ$

The signal of the shower on the ground is determined by the interaction of charged particles in the tanks. The total signal on the ground has distinct components and one can write the total signal as:

$$S_{total} = S_\mu + S_{em} + S_{em/\mu} \quad (3)$$

where all signals are given in Vertical Equivalent Muon (VEM) and they correspond to:

- S_μ is a muonic component
- S_{em} is a pure electromagnetic component
- $S_{em/\mu}$ is the electromagnetic component due to muon decay and muon interactions, also known as electromagnetic halo.

The surface detector samples only a part of the particles arriving at ground. In order to recover the total information given by a shower on the ground a fit to the lateral distribution has to be performed.

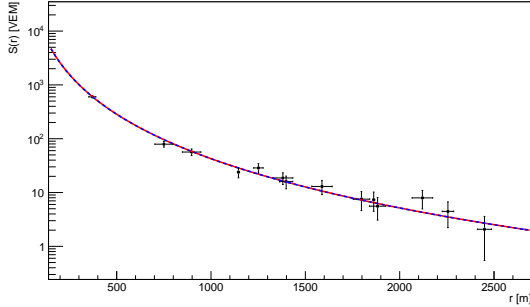


Figure 5: Example of an NKG Fit to the lateral distribution function for a simulated proton event at $\theta=60^\circ$ and $E=10^{19}$ eV. The black dots correspond to the position and signal in the triggered stations and respective error bars.

The function that gives a good description of the signal is the modified Nishimura Kamata Greisen (NKG) function [9, 10]. The lateral dependence of the signal measured in tanks is modeled with the NKG as

$$S(r) = S_{1000} \left(\frac{r}{r_{1000}} \right)^\beta \left(\frac{r + r_{700}}{r_{1000} + r_{700}} \right)^{\beta+\gamma} \quad (4)$$

where β , γ and S_{1000} are the fit parameters. In order to recover the total signal of a shower on the ground one has to compute the integral of $S(r)$.

For a shower front coming from a given direction θ , the number of muons entering the tanks is given by the product of the projected shower front area and the muon density. The total signal detected does not correspond to the energy deposited by the muons in the tank. Competing processes such as ionization and Cherenkov radiation take place in the water tanks. The PMTs only detect part of the energy deposit, corresponding to the Cherenkov photons. The signal detected corresponds to the Cherenkov photons emitted by the muons in the tank. The signal depends on the zenith angle θ , thus averaging on θ one can then write:

$$\langle S_\mu(\theta) \rangle = N_\mu \langle \hat{t}_\mu(\theta) \rangle = \rho_\mu A_\theta \frac{\langle t_\mu(\theta) \rangle}{t_\mu(0)} \quad (5)$$

where $\frac{\langle t_\mu(\theta) \rangle}{t_\mu(0)}$ is the mean track normalized. The mean track can be easily computed as:

$$\langle t_\mu(\theta) \rangle = \frac{\int t_\mu(x, y) dx_\theta dy_\theta}{\int dx_\theta dy_\theta} \quad (6)$$

$$= \frac{\int t_\mu dA_\theta}{\int dA_\theta} \quad (7)$$

$$= \frac{V_{tank}}{A_\theta} \quad (8)$$

where $t_\mu(x, y)$ corresponds to the track in the projected plane, and V_{tank} is the volume of the tank.

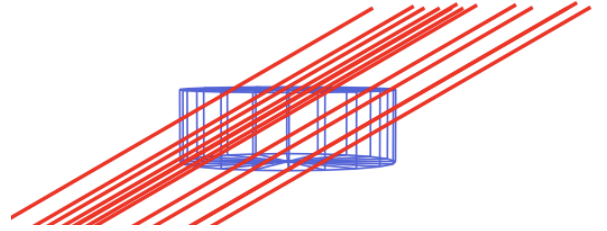


Figure 6: MC simulation of the tracks in an Auger tank for a $\theta = 60^\circ$ shower. The red lines correspond to the muon tracks.

Using the normalized mean track length we get:

$$\langle S_\mu(\theta) \rangle = \rho_\mu A_\theta \frac{\langle t_\mu(\theta) \rangle}{t_\mu(0)} \quad (9)$$

$$= \rho_\mu A_\theta \frac{V_{tank}}{A_\theta} \frac{A_0}{V_{tank}} \quad (10)$$

$$= \rho_\mu A_0 \quad (11)$$

where A_0 is the area of the top of the tank. The muonic density can be obtained from the fit to the LDF. Finally

we can determine the number of muons on the ground from the signal as follows:

$$N_{\mu} = \int_0^{2\pi} \int_R \rho_{\mu} r dr d\phi \quad (12)$$

$$= \frac{2\pi}{A_0} \int_{r_{min}}^{r_{max}} S_{\mu} r dr \quad (13)$$

where ϕ is the azimuthal angle, r is the distance to the shower axis in the perpendicular plane and N_{μ} corresponds to the number of muons on the ground. In expression 13 the integral on r can be evaluated for different limits. A systematic study was performed in order to determine which values to choose for r_{min} and r_{max} . The reconstructed number of muons will be compared to the number of muons from the MC simulation. From here one can do a study of the systematics in order to determine the performance of our method.

4.1 Application to Data

The method developed for recovering the number of muons on the ground can be applied to data from the Pierre Auger Observatory.

For the purpose of reconstructing the distribution of the data several cuts have to be applied. The method we developed only requires information from the SD. We will be using SD events collected at the Pierre Auger Observatory from 2004 to 2012. The cuts on the energy as well as on θ are given:

- $\log E$ [18.95 – 19.05]
- θ [58.5 – 61.5]
- 178 events pass all the cuts

Using the 178 events that passed our cuts one can apply the reconstruction method and plot the obtained distribution. Figure 7 shows the distributions for proton and iron primaries and also the one obtained for the data. Data has a mean value well above the predictions of the hadronic interaction model QGSJETII for proton and iron primaries in agreement with previous results [6]. We have shown that with a very simple model one can recover the distribution of the number of muons N_{μ}^{rec} . The values of the mean and RMS can be compared with the values of reference of the proton and iron distributions which allows mass composition studies and test of the hadronic interaction models.

The results obtained are neither compatible with proton nor with iron primaries for QGSJETII. Furthermore the study of the shape of the distributions could allow new insights into the shower properties.

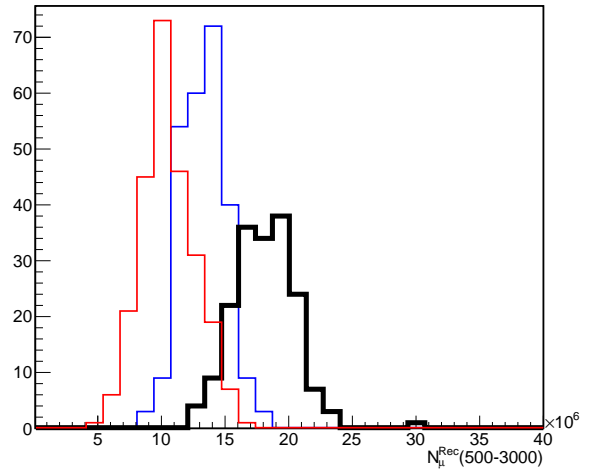


Figure 7: Distributions of N_{μ}^{rec} for proton (red) and iron (blue) for QGSJETII interaction model. In black one has the resulting distribution of N_{μ}^{rec} for the data.

Another important feature can be seen in the umbrella plots where we compare the RMS and the mean value for the number of muons for various models. Umbrella plots depict the phase space considering the transition from proton to iron primaries and considering also all the intermediate elements. All possible primaries from $A=1$ to $A=56$ are considered. One can locate our point within this plots in order to see if it is in agreement with any of the hadronic models and composition.

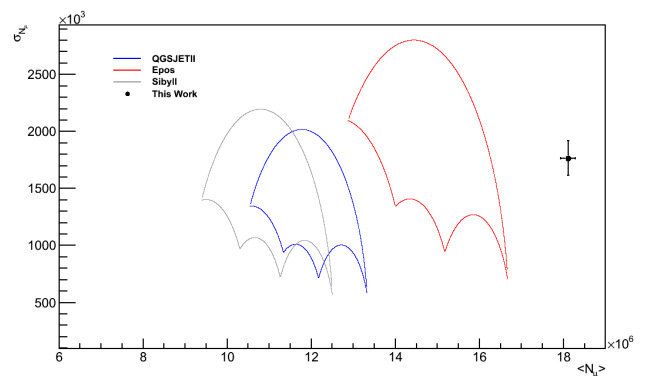


Figure 8: Umbrella Plot showing the phase space for the various models and the point we obtain using our method. The error bars correspond to the statistical error, the systematic error will be determined in future works.

In figure 8 we can see that the value obtained for the data is not compatible with any of the actual hadronic models.

The strength of this method relies on the simplicity of the transformations performed on the ground signal in order to recover N_{μ}^{rec} . The resolution event by event is slightly smaller than the width of the N_{μ} distribution and the separation of the proton and iron distributions. This property allows the study of the shape of the distribution, which has important physical information.

5 Conclusion

We studied in detail several scenarios composition scenarios, and also scenarios where we change the hadronic models. We conclude that current data cannot be fully explained by a bimodal change in composition. A transition from pure proton to pure iron is completely outruled from the $\text{RMS}(X_{\text{max}})$. An initial mixed composition accomodates the general features in the $\text{RMS}(X_{\text{max}})$ but the hadronic models would need further modifications in order to explain the trend in $\langle X_{\text{max}} \rangle$.

In the analysis of the cross-section scenarios we have seen that changing only one hadronic parameter, i.e. the cross section, accomodates many of the observed features, though the highest energy data would still be unresolved. This indicates that the hadronic models would need further modifications (multiplicity, inelasticity) in order to fit the actual data.

We have also provide a new original method to determine the number of muons on the ground N_{μ}^{rec} . A detailed study of the new method is provided and in the final part we apply the reconstruction to the available SD data.

In this analysis we find that the number of muons from the SD data is above the number of muons for any of the models and considering both iron and proton initiated showers. This is further strong evidence that the hadronic models do not give a good description

the real EAS data. Furthermore one can add that this new method provides the distribution for the number of muons N_{μ}^{rec} coming from the data. This distributions are relevant due to the fact that a study of their shape might provide new information concerning the physics of EAS.

References

- [1] T. Stanev, High Energy Cosmic Rays, Springer-Verlag (2004).
- [2] M. S. Longhair, High Energy Astrophysics, Cambridge University Press (2011).
- [3] James Cronin, Cosmic rays: the most energetic particles in the universe, Rev. Mod. Phys. (1999) **71**, 165.
- [4] Pedro Facal for the Pierre Auger Collaboration, The distribution of shower maxima of UHECR air showers, (2011), arXiv:1107.4804v1
- [5] J. Abraham et al., Measurement of the energy spectrum of cosmic rays above 1018 eV using the Pierre Auger Observatory, Phys.Lett., B685:pp. 239–246, 2010, doi:10.1016/j.physletb.2010.02.013, arXiv:1002.1975.
- [6] Gonzalo Rodriguez for the Pierre Auger Collaboration, Reconstruction of inclined showers at the Pierre Auger Observatory: implications for the muon content, Proceedings of the 31st ICRC (2011).
- [7] F. Ionita et al., Properties of the Xmax distribution, Pierre Auger GAP-Notes (2010), 2010-108.
- [8] R. Conceição et al., Proton-proton cross-sections: the interplay between density and radius, (2011), aXiv:1107.0912.
- [9] K. Kamata and J. Nishimura, Prog. Theoret. Phys. Suppl. 6, 93 (1958).
- [10] K. Greisen, Progress in Cosmic Ray Physics, volume 3, North-Holland, Amsterdam, 1956.